
Appendix for Paper 8410

Anonymous Author(s)
Affiliation
Address
email

1 Appendix

2 1.1 Open source

3 To replicate the training pipeline for the STGCN-3-256 model, please look into the attached folder
4 entitled "NEURIPS-LinGCN-cleaned". For your convenience, we have provided the model and test
5 code for the 4-STGCN-3-256 model in the aforementioned folder. Additionally, the test result logger
6 file can be located within the directory at "NEURIPS-LinGCN-cleaned\work_dir\tmp\log.txt". These
7 resources have been made accessible to promote clarity and ease of reproduction for those interested
8 in building upon this work.

9 1.2 HE encoding with AMA format

10 Prior to encoding input data into polynomials, it is necessary to map the four-dimensional tensor
11 $X \in R^{B \times C \times T \times J}$ to a one-dimensional vector in $R^{N/2}$ using the AMA format, as proposed in [1].
12 This transformation allows for more efficient execution of STGCN forward-computation in the HE
13 domain. Below, we present the definition of the *Vec* function employed to map tensor X to a vector
14 in $R^{N/2}$:

$$\begin{aligned} \text{Vec}(X) = y_j &= (y_{0,j}, \dots, y_{i,j}, \dots, y_{N/2,j}) \in R^{N/2} \\ \text{s.t. } y_{i,j} &= X_{((i \bmod T) \% B) \times (i \bmod B \cdot T) \times (i \% T) \times j} \\ & j \in J \end{aligned} \quad (1)$$

15 Following the mapping process, the vectors y_j are encoded into polynomials with degree N and
16 subsequently encrypted into ciphertext ct_j , as detailed in [2]. In this study, when N is set to 2^{16} ,
17 all tensors, including intermediate tensors, can be encrypted and packed into 25 ciphertexts, which
18 corresponds to the number of nodes. For cases where $N = 2^{15}$ (2^{14}) the number of ciphertexts
19 is 50(100). By selecting an appropriate value for N , the encryption and packing processes can be
20 optimized to maintain performance and efficiency.

21 1.3 HE Setting Details

22 In Table 1, we furnish comprehensive details regarding the HE inference parameters. Specifically,
23 i-STGCN-3 denotes a 3-layer STGCN model with i effective non-linear layers, while i-STGCN-6
24 signifies a 6-layer STGCN model with i effective non-linear layers. In this context, N represents the
25 polynomial degree, and Q corresponds to the coefficient modulus.

26 To guarantee computation precision utilizing a one-time rescale operation, we assign the scale factor
27 p for both ciphertext and plaintext to 2^{33} . This allocation results in a reduction of the current Q of
28 ciphertext by p bits. This setup ensures that the overall performance and accuracy conform to the
29 desired criteria while capitalizing on the security and resilience advantages conferred by HE.

Table 1: HE parameter settings in detail.

Model	Encryption Parameters				Mult Level
	N	Q	p	q_0	
6-STGCN-3	32768	509	33	47	14
5-STGCN-3	32768	476	33	47	13
4-STGCN-3	32768	443	33	47	12
3-STGCN-3	16384	410	33	47	11
2-STGCN-3	16384	377	33	47	10
1-STGCN-3	16384	344	33	47	9
12-STGCN-6	65536	932	33	41	27
11-STGCN-6	65536	899	33	41	26
7-STGCN-6	32768	767	33	41	22
5-STGCN-6	32768	701	33	41	20
4-STGCN-6	32768	668	33	41	19
3-STGCN-6	32768	635	33	41	18
2-STGCN-6	32768	602	33	41	17
1-STGCN-6	32768	569	33	41	16

Table 2: Comparison of latency breakdown between the non-reduced model with optimized model.

Model	HE Operators latency (s)				Total Latency (s)	Speedup (\times)
	Rot	PMult	Add	CMult		
6-STGCN-3-128	1336.25	378.25	99.65	37.45	1851.60	-
2-STGCN-3-128	392.21	266.13	68.90	14.31	741.55	2.50
6-STGCN-3-256	2641.09	1508.19	397.17	74.90	4621.36	-
2-STGCN-3-256	777.68	1062.21	274.96	28.63	2143.47	2.16
12-STGCN-6-256	18955.09	1545.09	396.23	275.39	21171.80	-
2-STGCN-6-256	4090.08	1006.79	244.19	115.05	5456.12	3.88

30 1.4 HE inference on GCNConv and Temporal-Conv Layer

31 Upon obtaining the AMA-packed ciphertexts ct_j , the adjacency matrix multiplication $A \cdot X$ can be
 32 decomposed into a series of plaintext multiplications, $PMult$, in the HE domain. This decomposition
 33 accelerates HE-inference without necessitating rotations. Furthermore, the subsequent temporal
 34 convolution is performed solely on the temporal dimension T , utilizing 1×9 kernels.

$$ct'_k = A \cdot X = \sum_{i=1}^m ct_k A_i = \sum_{i=1}^m \sum_{k=1}^J PMult(ct_{i_k}, a_{i_k k}) \quad (2)$$

35 The AMA-packed ciphertexts allow for natural temporal convolution by single-node ciphertext ct_j ,
 36 facilitating independent computation. This approach results in a ReLU-reduction design through
 37 structural pruning of ReLUs. The primary constraint to consider in this context is ensuring that the
 38 level consumption of each ciphertext remains equal prior to the GCNConv layer (node aggregation).

39 1.5 Further Detail of Operator Fusion

40 During the HE-inference process, employing weight fusion conserves the multiplicative depth,
 41 consequently reducing the ciphertext level budget. For instance, batch normalization, defined by
 42 an affine transformation $a'x + b'$, and a polynomial activation function, defined by $(ax + b)^2 + c$,
 43 can be readily fused into the corresponding temporal convolution layer $wx + b''$ with the function
 44 $w(a(a'x + b') + b) + b'' = (w \cdot a \cdot a')x + ab' + wb + b''$. As a result, three consecutive multiplications
 45 are consolidated into a single multiplication (pre-computing $w \cdot a \cdot a'$), thereby reducing the level
 46 consumption of ciphertext from 4 to 2 (1×9 convolution, batch normalization, and polynomial
 47 activation).

48 Analogous to the temporal-convolutional layer, the same fusion strategies can be applied to the
 49 polynomial activation and batch normalization of the GCNConv layer. Utilizing AMA-packed

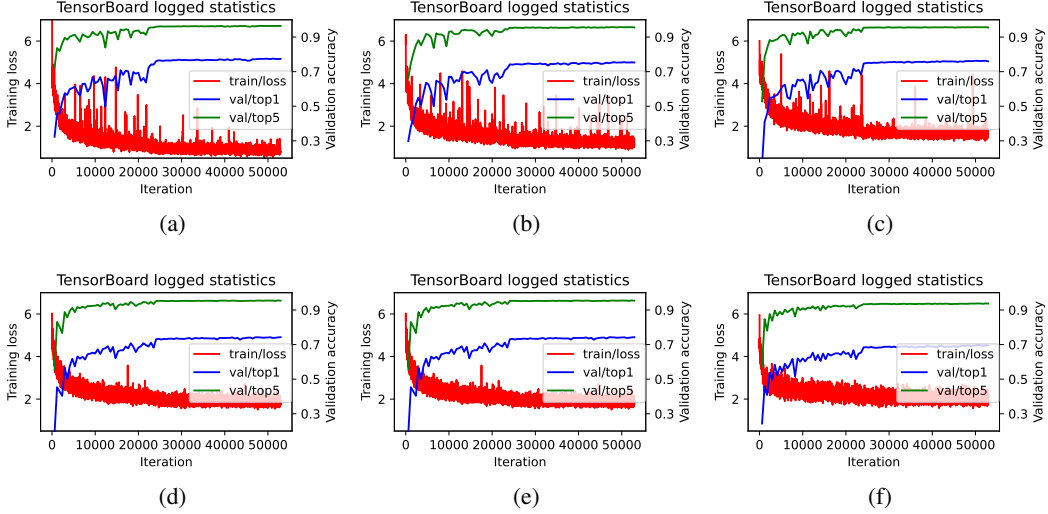


Figure 1: Polynomial replacement training curves for (a) 6-STGCN-3-128 (b) 5-STGCN-3-128 (c) 4-STGCN-3-128 (d) 3-STGCN-3-128 (e) 2-STGCN-3-128 (f) 1-STGCN-3-128

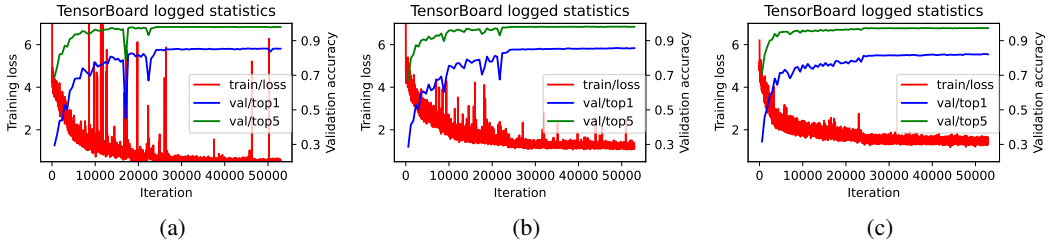


Figure 2: Polynomial replacement training curves for (a) 12-STGCN-6-256 (b) 4-STGCN-6-256 (c) 2-STGCN-6-256

50 ciphertexts, the node aggregation in GCNConv is translated as depicted in Equation 2, where each
 51 ciphertext carries out scalar multiplication with the plaintext of matrix elements $a_{i_k, k}$. Consequently,
 52 these plaintext matrix elements $a_{i_k, k}$ are fused with the primary 1×1 convolutional kernels to
 53 conserve the multiplicative level, reducing the total level consumption of the GCNConv layer from
 54 4 to 2 (1×1 convolution, adjacency matrix multiplication, batch normalization, and polynomial
 55 activation).

56 1.6 Operator latency breakdown

57 Table 2 presents a comprehensive operator latency breakdown encompassing Rot, PMult, Add, and
 58 CMult operations. The designation i-STGCN-3-128 refers to an STGCN-3-128 model with i residual
 59 non-linear layers. As indicated in the table, the non-linear reduction contributes to a significant
 60 reduction in latency. By leveraging a smaller polynomial degree N, the overall latency experiences
 61 substantial improvement.

62 1.7 More Training Details and Insight

63 In this section, we present the training curves for the STGCN-3-256 model, which employs 6 to 1
 64 effective second-order polynomial (non-linear) layers. Figures 1(a) through Figure 1(f) depict the
 65 training curve progression. During the training process, we utilized mixed-precision training for the
 66 polynomial model, which led to occasional instability in some iterations, as evidenced by spikes in
 67 the loss values. Nevertheless, the training process demonstrated rapid recovery following such loss
 68 spikes.

69 As demonstrated in training curve, a smaller number of second-order polynomial (non-linear) layers
70 contribute to a more stable training process and facilitate smoother convergence. This finding
71 explains the enhanced performance of the STGCN-6-256 model, which features a reduced number of
72 non-linear layers, as compared to the full-polynomial model baseline.

73 To substantiate our hypothesis, we plot the polynomial replacement training curve for the STGCN-6-
74 256 model in Figure 2. The training curves for 12 effective non-linear layers (12-STGCN-6-256), four
75 effective non-linear layers (4-STGCN-6-256), and two effective non-linear layers (2-STGCN-6-256)
76 are presented. As the number of non-linear layers increases, the model achieves greater expressivity;
77 however, the polynomial replacement process becomes increasingly unstable. Consequently, for the
78 STGCN-6-256 model with only 4 non-linear layers, a more stable replacement process facilitates
79 better convergence, ultimately leading to improved accuracy performance.

80 **References**

- 81 [1] Ran Ran, Wei Wang, Quan Gang, Jieming Yin, Nuo Xu, and Wujie Wen. Cryptogcn: Fast and
82 scalable homomorphically encrypted graph convolutional network inference. *Advances in Neural*
83 *Information Processing Systems*, 35:37676–37689, 2022.
- 84 [2] Jung Hee Cheon, Kyoohyung Han, Andrey Kim, Miran Kim, and Yongsoo Song. A full rns
85 variant of approximate homomorphic encryption. In *International Conference on Selected Areas*
86 *in Cryptography*, pages 347–368. Springer, 2018.